Original Paper

Cellular Physiology and Biochemistry

Cell Physiol Biochem 2011;27:281-290

Accepted: February 21, 2011

Optical Action Potential Screening on Adult Ventricular Myocytes as an Alternative QT-screen

Qinghai Tian[1], Martin Oberhofer[1], Sandra Ruppenthal[1], Anke Scholz[1], Volker Buschmann[2], Hidekazu Tsutsui[3], Atsushi Miyawaki[3], André Zeug[4], Peter Lipp[1] and Lars Kaestner[1]

[1]Institute for Molecular Cell Biology, Building 61, Saarland University, Homburg/Saar, [2]PicoQuant GmbH, Berlin, [3]Laboratory for Cell Function Dynamics, Brain Science Institute, RIKEN, Hirosawa, Saitama, [4]Cellular Neurophysiology, Hannover Medical School, Hannover

Key Words

Di-8-ANEPPS • Mermaid • Cardiac myocytes • Cardiac toxicity • QT-screen • Genetically encoded potential sensor

Abstract

Background/Aims: QT-interval screens are increasingly important for cardiac safety on all new medications. So far, investigations rely on animal experiments or cell-based screens solely probing for conductance alterations in heterologously expressed hERG-channels in cell lines allowing for a high degree of automation. Adult cardiomyocytes can not be handled by automated patch-clamp setups. Therefore optical screening of primary isolated ventricular myocytes is regarded as an alternative. Several optical voltage sensors have been reported for ratiometric measurements, but they all influenced the naïve action potential. The aim of the present study was to explore the recording conditions and define settings that allow optical QT-interval screens. Methods: Based on an improved optical design, individual action potentials could be recorded with an exceptional signal-to-noise-ratio. The sensors were validated using the patch-clamp technique, confocal microscopy and fluorescence lifetime imaging in combination with global unmixing procedures. Results: We show that the small molecule dye di-8-ANEPPS and the novel genetically encoded sensor Mermaid provide quantitative action potential information. When applying such sensors we identified distinctly different pharmacological profiles of action potentials for adult and neonatal rat cardiomyocytes. Conclusion: Optical methods can be used for QT-interval investigations based on cellular action potentials using either the small molecule dye di-8-ANEPPS or the genetically encoded sensor Mermaid. Adult cardiomyocytes are superior to neonatal cardiomyocytes for such pharmacological investigations. Optical QT-screens may replace intricate animal experiments.

Introduction

Action potential duration (APD) is believed to be a cellular equivalent to the QT-interval in the electrocardiogram [1]. Action potentials (APs) can be measured with two major approaches: either direct electrical measurement of voltages, e.g. by the patch-clamp method, or indirect measurements by molecular sensors. These sensors are probed by light and changes in photon responses are translated into values for the electrical (membrane)

KARGER

Fax +41 61 306 12 34
E-Mail karger@karger.ch
www.karger.com

1015-8987/11/0274-0281$38.00/0

Accessible online at:
www.karger.com/cpb

Lars Kaestner
Institute for Molecular Cell Biology, Building 61
Saarland University, 66421 Homburg/Saar (Germany)
Tel. +49 6841 16 26103, Fax +49 6841 16 26104
E-Mail anlkae@uks.eu

potential. Based on the patch-clamp method automated screens of properties of the heterologously expressed hERG channel in cell lines have been developed. They serve as a further reduced equivalent of QT-screens due to the guideline ICH Topic S7B [2] published by the EMEA and the FDA.

Because of their shape and fragility primary isolated adult cardiomyocytes cannot enter automated membrane potential measurements on patch-clamp robots. Instead contact-free optical approaches would be advantageous. So far procedures based on potentiometric dyes are lacking one or several of the following properties: (i) ability for quantification, (ii) sufficiently fast response time to follow APs, (iii) sufficiently high signal-to-noise ratio to avoid signal averaging, (iv) sensor-induced alterations of AP properties.

In this study we deployed a ratiometric read-out mode of di-8-ANEPPS up to a level that allows the registration of single cellular APs of adult or neonatal cardiomyocytes and hence the use of that method in automated high content approaches, such as QT-screens. Using this method we probed pharmacological alterations of neonatal and adult ventricular cardiomyocytes and demonstrate that APs in neonatal myocytes are an invalid model for the adult situation and thus application of these cells in pharmacological screens appears highly problematic.

Using adenoviral gene transfer [3] the detection technique was extended to one of the novel FRET based genetically encoded voltage sensor (GEVS), named Mermaid [4, 5]. This approach will allow the study of large cell populations especially under conditions of chronic electrical and/or pharmacological stimulation.

Materials and Methods

Photometric measurements

The optical system for measurements of APs is based on an inverted microscope (TE2000-U, Nikon, Tokyo, Japan). When using di-8-ANEPPS, a monochromator provided the excitation light beam (460 nm ± 7 nm; Polychrome IV; TILL Photonics, Gräfelfing, Germany) that was reflected by a dichroic mirror (centred at 485 nm), and guided to the dye-loaded cells through an immersion objective (40x/1.30 S Fluor - for adult cells; 20x/0.75 Plan Flour - for neonatal myocytes). The emitted fluorescence was initially cleaned with a 532 nm dichroic long pass filter (DCLP) and separated into two channels (580DCLP). Light detection was achieved with two avalanche photodiodes (TILL Photonics). The signals were sampled and digitised with a DSI-200 (IonOptix, Milton, USA) at 1 kHz and recorded with IonWizard Software (IonOptix) resulting in a recording time of 1 ms per data point. For the Mermaid measurements, the 532DCLP filter was removed and the 585DCLP was changed to a 532 nm dichroic mirror. Adult and neonatal myocytes were stained with di-8-ANEPPS as previously described [6] using a final concentration of 5 μM for 7 min and 10 min, respectively, in the presence of 2 μL test compound stock solution, when needed. The following substances were used as test drugs: (2 ethenyl-4-azabicyclo [2.2.2] oct-5-yl)-(6-methoxyquinolin- 4-yl)-methanol (quinidine), 4-aminopyridine (4-AP), and 1-[2-(6-methyl-2-pyridyl)ethyl]-4-(4-methylsulfonyl-aminobenzoyl)piperidine (E-4031) - all purchased from Sigma-Aldrich (Heidenheim, Germany). Afterwards the cells were washed with fresh Tyrode containing the same concentration of test compound. Then the cells were placed on the microscope, field stimulated (0.5 Hz from a field stimulator (MyoPacer, IonOptix)). The illumination as well as the detection area was restricted by a rectangular adjustable aperture covering an individual cell at a time. For measurements contracting cells were randomly chosen.

The photometry data were analysed in Igor Pro software (WaveMetrics, Oregeon, USA) with custom-made macros calculating the AP duration at 70% repolarisation (APD_{70}). For the compounds tested, resulting APD_{70}s for different concentrations were fitted within GraphPad Prism (GraphPad Software, La Jolla, USA) and the final IC_{50} values were calculated. The number of cells tested is assigned by „n“, whereas independent preparations/animals allocate to „N“.

Isolation of adult and neonatal cardiomyocytes

Cardiomyocytes were isolated from male Wistar rats (Charles River, Sulzfeld, Germany). Adult cardiomyocyte isolation and culture was executed on 7 weeks old rats having a body weight of approximately 250 g as stated elsewhere [7]. Di-8-ANEPPS measurements were performed on freshly isolated cells, while Mermaid measurements were performed after 2 days in culture (see below).

For the isolation of neonatal cardiac myocytes 4-6 neonatal or one day old rat pups were anaesthetised with ice and killed by decapitation, and the hearts were removed and put into ice-cold isolation buffer (in mM: 116 NaCl, 20 HEPES, 0.8 Na_2HPO_4, 5.6 glucose, 5.4 KCl and 0.8 $MgSO_4$, pH 7.35). The hearts were washed once with isolation buffer and segmented into 0.5 mm^3 pieces. The tissues were transferred to an enzyme-mix comprising isolation buffer with 0.6 mg/mL Pankreatin (P3292, from Pocine Pancreas, Sigma-Aldrich, Heidenheim, Germany) and 0.4 mg/mL Collagenase Type II, and incubated in a 37°C water bath with gentle agitation for 20 min. The resulting supernatant from the first digestion was discarded. Then the heart tissue was digested for another 5 times as described above. Every time, the resulting supernatant was collected, centrifuged (600 g for 5 min) and immediately resuspended in F10 complete medium (Invitrogen GmbH, Karlsruhe, Germany) containing 10% horse serum (Fisher Scientific GmbH, Schwerte, Germany), 5% FCS (PAA Laboratories, Linz, Austria) and 100 μg/mL. Penicillin/Streptomycin. The cell populations harvested in that way were combined, plated into a 75 cm^2 flask, and incubated for 2 hours at 37°C. Thereafter the supernatant was collected carefully, centrifuged as described above and the

remaining cell pellet was resuspended in F10 complete medium. The cells were counted and plated onto cover slips coated with an extracellular matrix protein mixture (Sigma-Aldrich) in 12-well plates at a density of $5x10^4$ cells per well. The neonatal cardiac myocytes were cultured in an incubator at 37°C with a 5% CO_2 atmosphere, and the medium was changed at DIV1 (day *in vitro*), DIV3 and DIV5.

Measurements of single cell emission spectra and patch-clamp measurements

CHO/KCNH2 cells (kindly provided by Dr. Udo Kraushaar, NMI Reutlingen, Germany) growing on coverslips were loaded with di-8-ANEPPS. Compared to cardiac myocytes dye loading was slightly enhanced (10 µM for 10 min in Tyrode) to achieve a photon count allowing for spectral resolution. The CHO cells were transferred onto the stage of a Nikon TE2000-U microscope and excited at 460 nm. Emission spectra from individual cells were recorded with a spectrometer (USB2000, OceanOptics, Ostfildern, Germany) either in standard Tyrode (5.4 mM KCl) or in depolarising solution (in mM: 25.4 NaCl, 120 KCl, 10 glucose, 10 HEPES, 1.8 $CaCl_2$ and 1 $MgCl_2$, pH 7.35). The settings of the spectrometer were kept constant in between the measurements (integration time 500 ms, no spectrum average).

Patch clamp recordings were performed as previously described [8].

Confocal recordings and 3D reconstruction

Forty-eight hours after virus infection, the medium for the adult ventricular myocytes was changed to a Ca^{2+}-free solution (140 NaCl, 5.4 KCl, 10 glucose, 10 HEPES, 10 EGTA, 1 $MgCl_2$, in mM: pH 7.35) and they were transferred onto the stage of a confocal microscope (TCS SP5 II, Leica, Mannheim, Germany), where imaging was performed using a 63x/1.4 objective (HCX PL APO). After deconvolution of the raw data with AutoDeblur Software (AutoQuant, Media Cybernetics, Bethesda, USA), the data were imported into Imaris (Bitplane AG, Zurich, Switzerland) for 3D reconstruction by surface rendering.

Mermaid measurements

Adenoviruses encoding for Mermaid were constructed as described before for genetically encoded calcium sensors [9]. The pcDNA3-Mermaid vector entering the virus production was described elsewhere [4]. Virus amplification and the transduction procedure were described in details previously [7]. Immediately after isolation, the cardiomyocytes were infected with an adenovirus encoding for Mermaid (multiplicity of infection of 20) for 12 hours. Transduction efficiency was above 80% and cardiomyocyte survival was not affected. Forty-eight hours after infection, cells were treated with 20 mM 2,3-Butanedione 2-monoxime (BDM, Sigma-Aldrich) for 10 min before recording. The experiments were performed on a microscope that was enclosed in a 37°C climate box that also housed all preheated experimental solutions. When applying test substances, we monitored three stimulations prior to the administration and three stimulations 2 minutes after drug administration. Cells were electrically paced during the entire experimental procedure to ensure steady state conditions.

FLIM measurements and global unmixing procedurs

Fluorescence lifetime imaging (FLIM) measurements were performed on a confocal microscope equipped with a custom made FLIM upgrade. A picosecond pulsed white light laser (Femtopower1060 SC-430-4, Fianium, Southampton, UK) provided excitation light after passing through a 470/40 filter. This filter was selected since bleaching of Mermaid is reduced at wavelengths above 450 nm. Image generation was performed on a confocal scan-head (PCM2000, Nikon) attached to an inverted microscope (TE2000, Nikon). For detection the light was separated into 2 channels (505DCLP primary dicroic; 565DCLP secondary dicroic) and cleaned up by 515-555 nm and 570-640 nm emission filters. The spectral channels were chosen to reach a similar photon count for Mermaid in both channels for a given excitation wavelength. Light was detected by photon counting avalanche photodiodes (PDM series, Micro Photon Devices, Bolzano, Italy). Photon counting was performed by a two channel HydraHarp controlled by SymPhoTime software (PicoQuant, Berlin, Germany).

Reference measurements of the fluorescence lifetime with cells expressing Mermaid and cells labelled with di-8-ANEPPS were performed under experimental conditions as described above. Their global fluorescence lifetime trace was fitted by the convolution of the device response function with mono- and double-exponential decays. Due to unavoidable artefacts in the device response function better fitting results were obtained by approximating the device response by a Gaussian function. Thus the convolution integral could be reformulated as:

$$F(t) = \sum_i A_i \, Exp\left(\frac{\sigma^2 + 2\tau_i (t_0 - t)}{2\tau_i^2}\right) Erfc\left(\frac{\sigma^2 + \tau_i (t_0 - t)}{\sqrt{2}\sigma\tau_i^2}\right) \quad (1)$$

A_i and τ_i being the amplitude and the fluorescence decay time of the corresponding fluorophore and σ and t_0 being the half width and time point of the Gauss shaped device response.

In similarity to a previously introduced spectral unmixing concept [10], the FLIM data of the double labelled cells were linearly unmixed on a pixel-by-pixel based manner using reference time traces generated by equation (1) with the fluorescence lifetimes and relative amplitudes from reference measurements using single fluorophores. The required half width and time point of the Gauss shaped device response was obtained by a global fit of the fluorescence signal obtained from double-labelled samples, similar to the reference fitting procedure.

Results

Optical recording of genuine APs in individual cardiac myocytes

Previously, we showed the application of ANEPPS dyes for the confocal detection of APs in isolated cardiomyocytes [11, 12]. For this study we have chosen

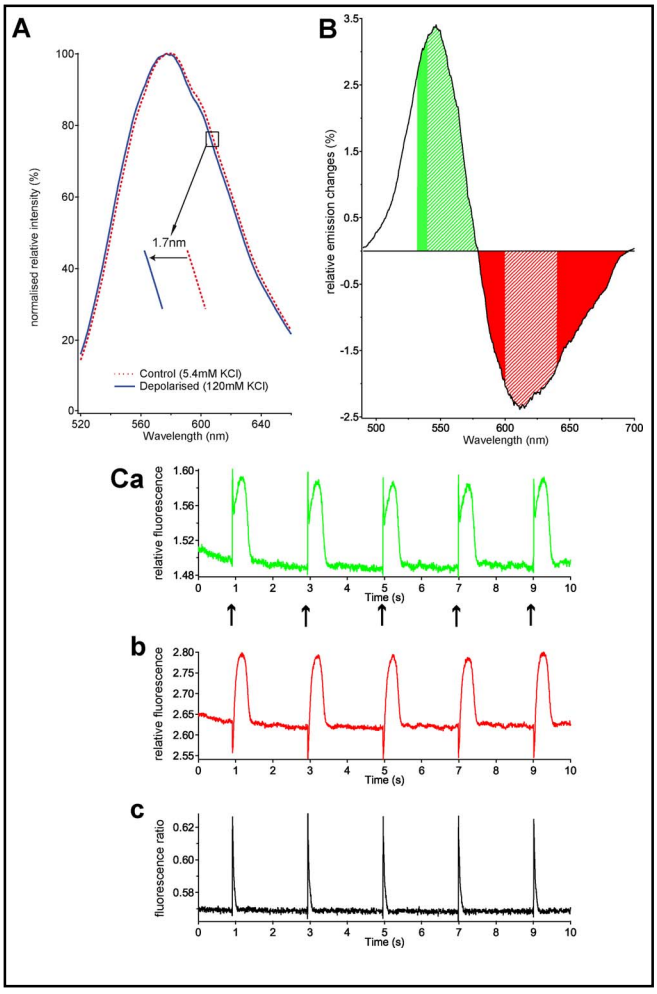

Fig. 1. Recording mode of the individual APs. (A) The spectra of di-8-ANEPPS loaded CHO/KCNH2 cells in low (5.4 mM) and high (120 mM) potassium (corresponding to a Nernst potential change of 83 mV) were measured and normalised. The difference in the spectra is shown in (B). The area under the curve represents the change in photon count for the green and red channel. The respective colour coded area indicate the measured spectral parts, whereas the hatched areas represent spectral channels of previous investigations (e.g. Hardy et al. [14]). With the avalanche photodiode-based photometry set-up, the green channel (532-580 nm), the red channel (580-700 nm) and the ratio signal (green divided by red) from individual rat adult ventricular myocyte are shown in (Ca), (Cb) and (Cc), respectively. The arrows in (Ca) indicate the time points of the electrical field stimulation.

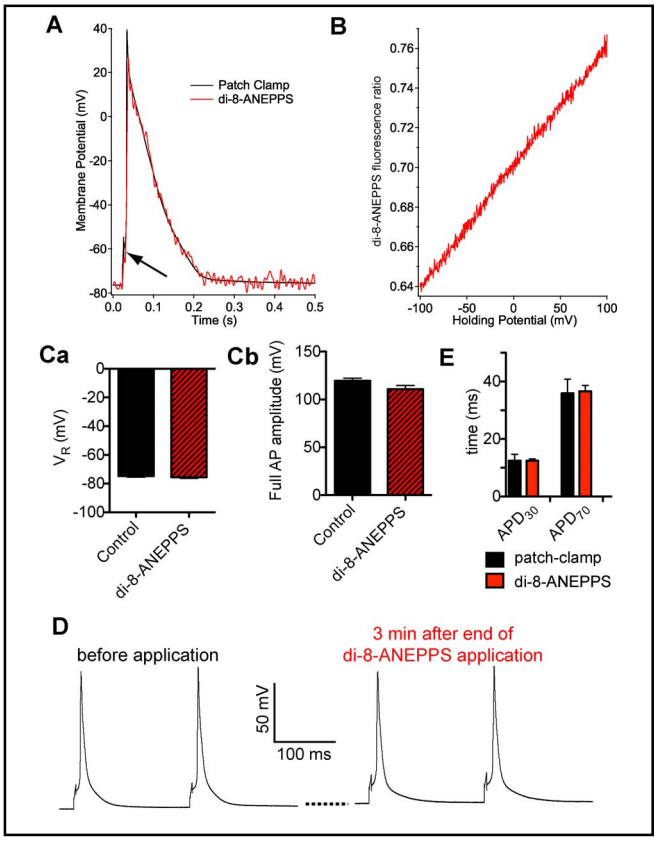

Fig. 2. Evaluation of di-8-ANEPPS on adult cardiomyocytes. (A) Correlation between the fluorescent signal and the patch-clamp signal. After a small current (600 pA) was injected into an adult cardiomyocyte via the patch pipette (indicated by the arrow), the fluorescent signal of di-8-ANEPPS and the real AP were recorded simultaneously by a photometric system and a patch-clamp system, respectively. (B) The calibration of the di-8-ANEPPS ratio signal. After a cardiomyocyte was patched successfully, a voltage ramp from -100 mV to +100 mV was applied on the cell in two seconds, and the fluorescent signals were recorded with the photometric system. Over the entire range the fluorescence ratio is linear to the membrane potential. (C) Comparison of the effect of di-8-ANEPPS itself on the cardiomyocytes' resting potential (VR) and AP amplitude (both parameters were read out by the patch-clamp technique); n=12. (D) shows representative APs before and 3 min after the di-8-ANEPPS loading procedure. (E) compares the AP duration (APD_{30} and APD_{70}) between optically measured cells (n=214) and unstained cells measured with the patch-clamp method (n=94).

di-8-ANEPPS because of its extremely low rate of internalisation (even after 60 minutes of dye loading there was no detectable intracellular fluorescence; data not shown) as well as its fast response kinetics.

For neurones and cardiomyocytes, it was reported that di-8-ANEPPS could be readout in a ratiometric manner [13, 14]. Here we show the spectral hypsochrome shift (approximately 1.7 nm) that occurs in di-8-ANEPPS-loaded living cells upon depolarisation (Fig. 1A; nominal voltage step: 83 mV). Complementary, Fig. 1B shows the difference of the two spectra provided in Fig. 1A. The coloured regions depict the spectral bands of the two channels measured by us and others (for details see figure legend).

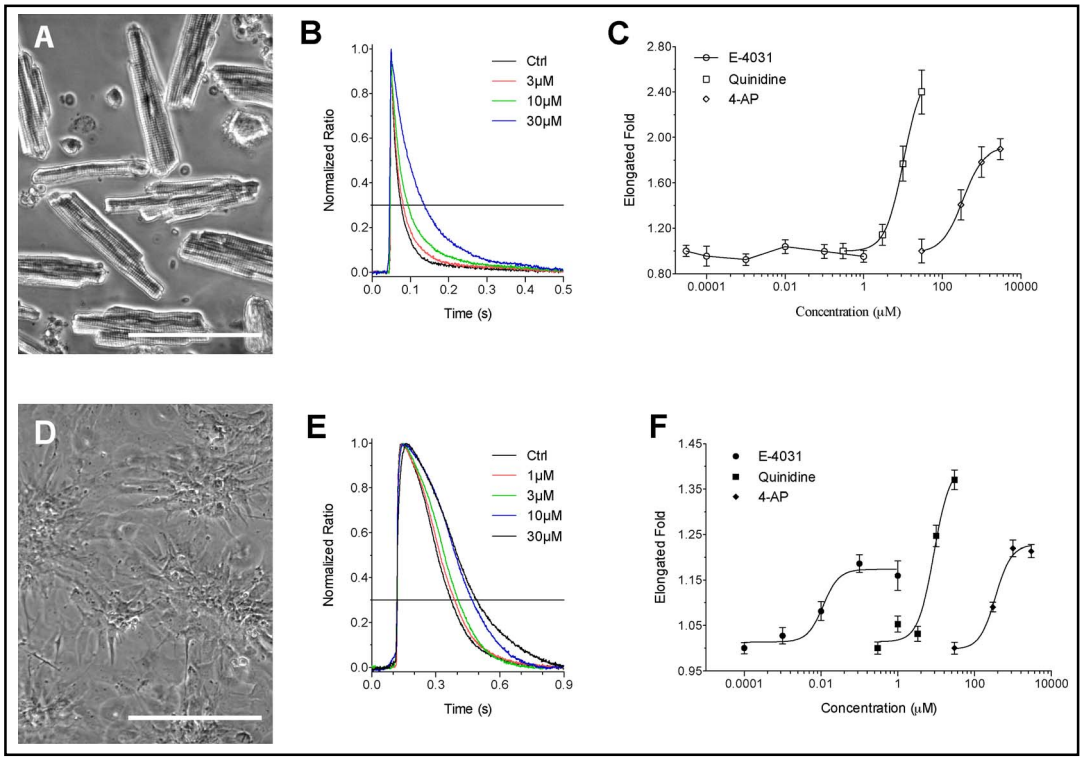

Fig. 3. Comparison of APs of neonatal and adult cardiomyocytes by optical recordings with di-8-ANEPPS. Panels (A) and (D) depict typical cells of adult and neonatal cardiac myocytes, respectively. The scale bar in the images represents 100 µm. The average APs of adult cardiomyocytes (B) and neonatal cardiomyocytes (E) in different concentrations of quinidine are shown. 20 to 30 cells from the same rat cardiomyocyte preparation were measured, averaged and normalised for each concentration in the curves depicted in (C) and (F). The effects of the three agents quinidine, E-4031 and AP-4 on APD_{70} are compared on rat adult (C) and neonatal cardiomyocytes (F). APD_{70} are plotted as mean ± SEM. The data were averaged from N=3 independent cell preparations for neonatal as well as for adult cardiomyocytes.

We have majorly improved the setup for optical recording of APs to obtain fluorescence data by using avalanche photo diodes instead of photon multiplying tubes and optimised dichroic and emission filters to record an increased spectral range (cp. Fig. 1B). The very high signal-to-noise ratio allows recording of individual APs and the detailed analysis of the fluorescence data.

The effect of the improvements can be deducted from Fig. 1C, that displays exemplified raw fluorescence recordings (Fig. 1Ca&b) and the resulting fluorescence ratio (Fig. 1Cc) for a single cardiac myocyte loaded with di-8-ANEPPS during a train of depolarising field stimulations (black arrows). While the raw fluorescence signals comprise the membrane voltage signals (initial upward or downward peaks) convoluted by the secondary contraction hump, the ratio-signal (Fig. 1Cc) only displays optically recorded membrane potential signals (at 1 kHz detection frequency).

Especially for quantitative optical recordings it is imperative to know (i) the quantitative relationship between the parameters probed and the resulting data and (ii) the degree to which a given sensor alters the cellular signals. Fig. 2 summarises data addressing both questions. For direct validation of the linearity between the di-8-ANEPPS fluorescence and the membrane potential, we combined simultaneous optical and electrophysiological recordings of APs, the results of that series of experiments is summarised in Fig. 2A-D. Fig. 2A depicts that the AP recorded electrophysiologically (black trace) is superimposable onto the fluorescence signal (red trace), indicating that di-8-ANEPPS is indeed fast enough to follow the rapid voltage changes. Even the stimulation artefact (current injection via patch pipette ~3 ms) was detected by the dye (black arrow in Fig. 2A). To further support the linearity between the membrane potential and the di-8-ANEPPS ratio, we generated voltage ramps (from -100 mV to +100 mV) and simultaneously recorded the di-8-ANEPPS signals. The relationship between both parameters was found to be linear (Fig. 2B).

Previously, Hardy and co-workers have reported changes of the AP properties after application of di-8-ANEPPS [14]. Due to our increased recording sensitivity loading of di-8-ANEPPS could be reduced to such a minimum (5 µM for 7 min) that APs before and after di-8-ANEPPS administration were indistinguishable (Fig. 2C&D). Under both conditions, the resting membrane potential (Fig. 2Ca), the AP amplitude (Fig. 2Cb) and APD_{30} as well as APD_{70} (Fig. 2E) were not changed. Original AP tracings before (Fig. 2D left) and 3 min after di-8-ANEPPS staining (Fig. 2D right) substantiated such findings.

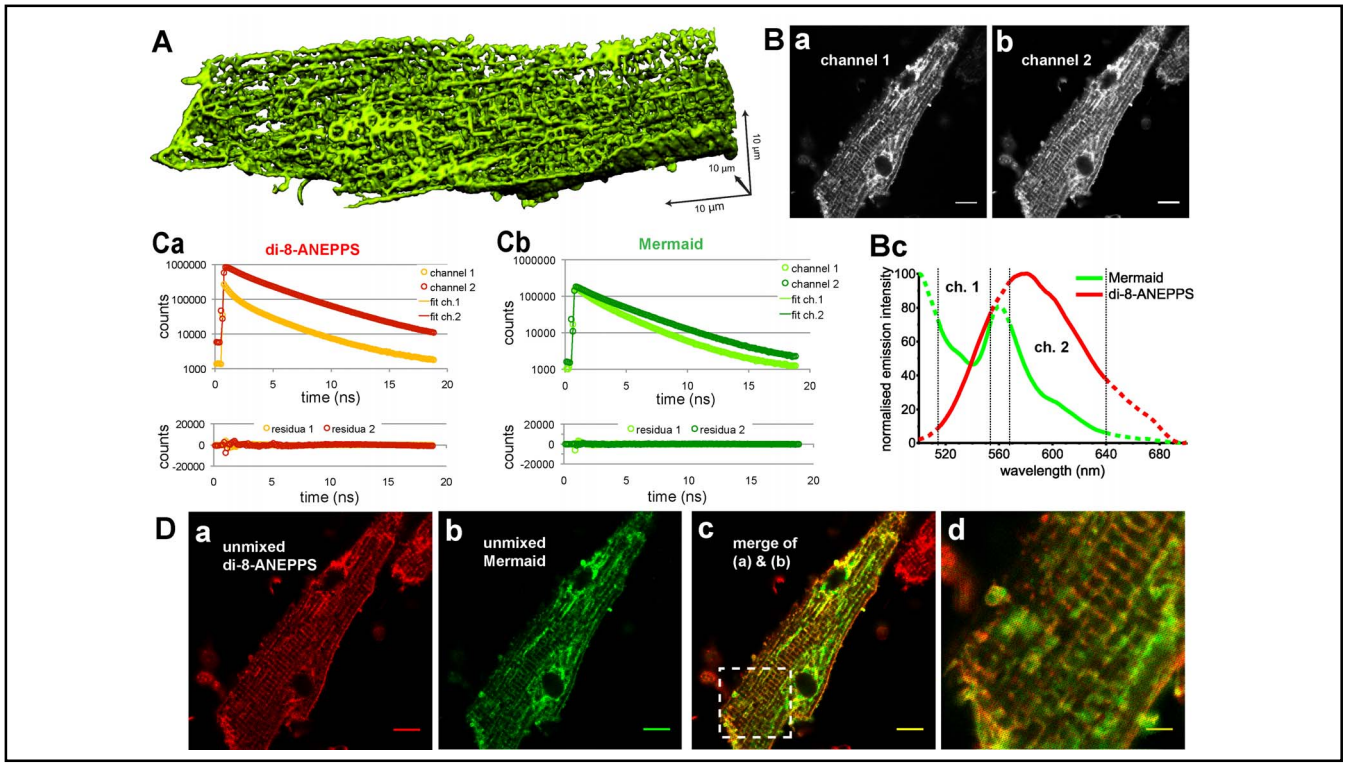

Fig. 4. Membrane localisation of Mermaid. (A) Example of the 3-dimensional distribution of the Mermaid protein in adult ventricular myocyte. The scale bars represents 10 µm in each direction. (B) raw images of a double stained cell in two spectral channels. Panel (Bc) depicts the spectral bandwidth of the channels in comparison to di-8-ANEPPS and Mermaid relative fluorescence intensities. The fluorescence lifetimes of di-8-ANEPPS and Mermaid were determined for the two channels in single stained cells. Representative lifetime curves are plotted in panel (Ca) and (Cb) for di-8-ANEPPS and Mermaid, respectively. (Da) and (Db) show the unmixed images for di-8-ANEPPS and Mermaid, respectively, whereas (Dc) displays the overlay of the images (Da) and (Db). The region of the dashed square was rescanned at a higher magnification and the unmixed channels were merged in image (Dd). The scale bar is 10 µM in images (Ba&b), (Da-c) and 3 µM in image (Dd).

Drug-induced AP prolongation in adult and neonatal cardiomyocytes

A major aim of this study was to investigate whether the optical approach for AP recording was applicable to large volume experimental series not only on the laboratory scale but also for pharmaceutical or safety screens as a cellular substitute for QT-interval screens [1].

To probe whether the electrophysiological properties of neonatal cardiac myocytes might be different to the adult situation the optical approaches introduced above was used to perform a basic „pharmacological profiling" of both cell types with three different well characterised substances that influence APD in a predictable way: quinidine [15-18], E-4031 [19, 20] and 4-AP [21, 22].

Fig. 3 summarises our results. Fig. 3A&D depict the typical brick-like morphology and fibroblast-like shapes of adult and neonatal myocytes, respectively. As exemplified in Fig. 3B quinidine application resulted in a concentration dependent prolongation of APs. Similar recordings were generated for 4-AP and E-4031. Since these substances are known to mostly affect repolarisation [15-22], we quantified changes of APD by measuring APD_{70} (horizontal line in Fig. 3B) and replotted a dose-response curve (Fig. 3C). While quinidine and 4-AP led to a significant prolongation of the adult ventricular myocytes´ APs, E-4031 failed to do so. When we analysed the neonatal myocytes under identical conditions (Fig. 3E&F), we found that the neonatal AP was vastly different from the adult one (compare Fig. 3B&E). Despite the fact that the maximal AP prolongation was reduced by almost a factor of two (Fig. 3D&F, compare 4-AP and quinidine), E4031 displayed a clear prolongation of the APD_{70} values for neonatal myocytes in contrast to the adult situation.

Application of the genetically encoded sensor Mermaid in adult cardiomyocytes

Chronic experiments or experiments that occupy many days require re-staining of the same population of cells. A procedure that might be accompanied by nega-

tive side effects for the cells. Instead, the application of a GEVS would be advantageous. Recently, a number of sensors based on a voltage-sensitive domain followed by a tandem of fluorescent proteins was introduced [4, 23, 24]. Out of these sensors we choose Mermaid because it was already successfully applied in neonatal cardiac myocytes [4] and zebrafish [5] to record APs. We have cloned the Mermaid cDNA into an adenoviral expression system.

Since previous reports about GEVS reported major problems concerning their location in the plasma membrane [25], we aimed for a detailed investigation of the plasma membrane localisation of Mermaid. At day 3 *in vitro* (DIV3), we analysed the subcellular distribution to verify proper localisation of the GEVS. Fig. 4A displays a representative 3D-reconstruction of part of a ventricular myocyte. Mermaid appeared to localise in the T-tubular membrane system in ventricular myocytes. Although this 3D-reconstruction strongly suggested a preferential localisation of the protein to the plasma membrane, we used another approach to quantitatively analyse the localisation of Mermaid. We compared the distribution of Mermaid fluorescence with that of di-8-ANEPPS. For this we employed global unmixing from fluorescence lifetime imaging data distributed over 2 spectral channels for each of the dyes. Representative lifetime traces are given in Fig. 4C. While the fluorescence decay for di-8-ANEPPS displayed bi-exponential time courses for channel 1 (τ: 0.74 ns and 3.45 ns) and channel 2 (τ: 1.28 ns and 3.76 ns), Mermaid fluorescence decay was only bi-exponential in channel 1 (τ: 1.25 ns and 3.08 ns) while channel 2 showed a mono-exponential time course (τ: 3.35 ns) - compare Fig. 4C. Fig. 4Da&b depict the di-8-ANEPPS and Mermaid distribution after global unmixing. When we overlaid both data (Fig. 4Dc) we could identify common and non-common features in both distributions. While for the cross-striated pattern, representing the T-tubular plasma membrane system, co-localisation for the dye and the protein was very good, Mermaid appeared to label some additional structures inside the myocyte (see also Fig. 4Db). Co-localisation analysis revealed a correlation factor of 0.83. Thus, around 17% of the fluorescence originates from structures that are not connected to the extracellular space and therefore do not contribute to the voltage dependent changes of the Mermaid signal. Instead, they largely contributed to contraction-dependent movement artefacts that in contrast to di-8-ANEPPS (see Fig. 1C) did not „ratio out“ entirely. Consequently, we suppressed contraction by 20 mM BDM, a compound well known for suppressing contractile responses in cardiac muscle [26]. In addition we found that in cardiomyocytes upon depolarisation at room temperature, Mermaid fluorescence did not display any change, despite contractile responses (data not shown). Increasing the temperature to 37°C restored the expected behaviour. Consequently, we performed all experiments involving Mermaid as well as the direct comparison to di-8-ANEPPS at 37°C.

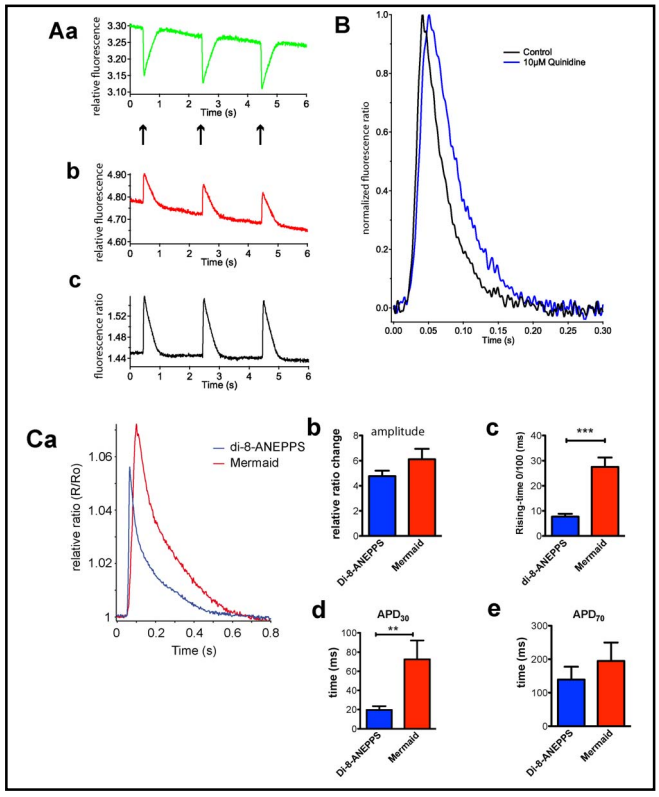

Fig. 5. Measuring APs with Mermaid. (A) Mermaid signals from single cells are shown (490-532 nm in (Aa), 532-700 nm in (Ab), and the resulting ratio in (Ac)). The arrows in (Aa) indicate the time points of the electrical field stimulation. (B) APs measured with Mermaid-expressing cells before and after application of 10 µM quinidine. (C) Comparison of APs from di-8-ANEPPS loaded cells (n=7) and from Mermaid transfected cells (n=4). In panel (Ca) representative APs of di-8-ANEPPS and Mermaid are plotted. Panels (Cb), (Cc), (Cd) and (Ce) depict the statistical analysis of the amplitude, the rise time the APD_{30} and the APD_{70}, respectively.

Field stimulation of Mermaid expressing myocytes resulted in the expected fluorescence changes for the green and red channel (see Fig. 5Aa&b, respectively). Despite noticeable bleaching in each individual fluorescence channel, the ratio displayed a stable baseline. Signal-to-noise ratio was that good that individual APs could be identified from an individual myocyte. Nevertheless, an important question remained: Is it possible to detect changes of AP parameters with Mermaid, similar to the

approach we have used for di-8-ANEPPS. For this we have recorded APs of individual myocytes before and after application of 10 µM quinidine, a concentration that prolonged APD significantly (see Fig. 3C). Fig. 5B displays a typical result of such recordings. On average, APD_{70} was increased from 116±12 ms before to 204±22 ms after application of quinidine.

Finally we compared the performance of di-8-ANEPPS and Mermaid to record APs on the same batch of cells under the same conditions, which are exemplified in Fig. 5C. It is obvious that Mermaid can follow APs in myocytes. Its ratio change is about 25% higher than that of di-8-ANEPPS (Fig. 5Ca&b). Especially the rising time is prolonged (Fig. 5Ca&c): 27.5±3.8 ms for Mermaid is more than 3½ times longer than that for di-8-ANEPPS (7.7±1.1 ms). For the decay time the APD_{30} shows significantly differences (Fig. 5Cd) whereas for APD_{70} the difference is not significant (p=0.42).

Discussion

In this study we have shown that APs of contracting cardiomyocytes can be optically measured in a ratiometric manner. Our approach allows optical recording of single APs without alterations of the naïve AP. Previous studies employing a ratiometric approach either used very high concentrations of di-8-ANEPPS (up to 100 µM vs. 5 µM in this study) [13] or required averaging of at least 10 to 20 APs before analysis [14]. This originated from technical improvements of our setup. Nevertheless, the patch-clamp technique still remains the more powerful approach when considering characterisation of membrane currents and single channel activity. For the investigation of APs, optical recording techniques might indeed proof superior since they enable larger numbers of cells to be analysed in any given time period. In addition, optical recordings leave the cell in a more undisturbed state, even in comparison to perforated patch approaches. The possibility to measure individual naïve APs opens up novel applications: (i) arrhythmic behaviour can - due to the lack of necessity for averaging - be observed nicely on the cellular level, and (ii) even minute alterations in the AP properties (such as duration) can be resolved. This will allow transfer of our approach to precise cardiac safety screens according to FDA and EMA requirements [1, 2]. We have recently demonstrated the possibility of an integration of adult cardiomyocytes into a high-content screening compatible workflow [27]. However, neonatal cardiomyocytes are a popular cell model, especially because cell isolation and handling is much easier compared to the adult situation. In contrast to the apparent ease of use, the obviously different shapes in adult vs. neonatal AP (compare Fig. 3B&E) render interpretation of neonatal data rather complex, especially when attempting to transfer neonatal data into the adult situation. This holds particularly true when considering pharmacological profiling of APs. We have demonstrated that by applying three different pharmacological tools known for the broad but rather defined action on membrane currents: quinidine, 4-AP, and E-4031.

Quinidine is a rather broad inhibitor since it blocks I_{Na}, I_{Ca}, I_{Kr}, I_{Ks}, I_{KI}, [15] I_{KATP} [16] and I_{to} [17, 18]. Quinidine´s IC_{50} of 10.36 µM measured optically (Fig. 3C) was in good agreement with electrophysiological data [28]. Nevertheless, the magnitude of the neonatal response was almost 4-fold smaller when compared to adult responses, despite similar apparent EC_{50} values.

Another agent known to prolong the cardiac action potential, 4-AP, is a potassium channel blocker with a relative selectivity for KCNA-channels [22]. Similarly to other studies [29], our data also demonstrated that 4-AP only had a small effect on the AP duration in neonatal cells. This was in clear contrast to adult myocytes, where 4-AP exhibited a massive prolongation of APD_{70} (25% vs. 100%; neonatal vs. adult).

Comparing an inhibitor for hERG-channels, E4031, a class III antiarrhythmic drug [20] revealed that AP was significantly prolonged (APD_{70}) in neonatal cardiomyocytes, while adult APs displayed no significant change (compare Fig. 3C&F). Such a behaviour can be explained by differences in the expression pattern especially for channels displaying outward K^+-currents, which is vastly different between neonatal and adult myocytes [30]. The neonatal AP displayed a much longer duration, which is in very good accordance with data published previously [31]. It has been reported that outward rectifying K^+-currents show a significantly lower current density (up to a factor of 10) in the neonatal myocytes when compared to the adult situation [31]. Starting from there, K^+-channel inhibitors such as those used in our study ought to exert larger effects in adult than in neonatal myocytes. We can conclude so far that neonatal cardiac myocytes are by no means an appropriate cell model for APs in adult cardiomyocytes.

It becomes even more surprising to realise that the state-of-the-art gold standard for cardiac safety screens, the hERG-expressing cell line (such as HEK293 cells) [32], does not even produce APs and only expresses a single major K^+-channel important for shaping APs in

cardiac myocytes. Especially repolarisation of the APs is a rather complex process to which a plethora of ion currents contribute to. These currents are expressed and regulated differently in the neonatal vs. adult situation. Thus hERG channel screen might allow very high throughput screens for pharmacological effects on that particular channel, but it is by far not the only important K^+-channel contributing to the AP repolarisation shape [33]. We are aware that rodent cardiomyocytes are no appropriate models for the human situation concerning cardiac safety as stated in the FDA/EMEA guidelines [2]. Here we just point out the differences between adult and neonatal cardiomyocytes. Nevertheless, the introduced procedure can be performed on other species including human isolated cardiomyocytes [9].

Even classical arguments against using adult cardiac myocytes such as standardised isolation or short-term culture have been solved recently. We have shown that reproducible and reliable isolation of adult ventricular myocytes is possible [7].

In our report, we have revealed a possible solution for another shortcoming of small molecular voltage sensors; loading the dyes into the cells has to be repeated when chronic and repeated measurements were to be performed on the same population of myocytes over the time course of day(s). Although loading of di-8-ANEPPS is quick, repeated application of this dye might exert unwanted side effects. We have shown, that the application of Mermaid, might overcome exactly that problem. With Mermaid, the recording of individual APs with a sufficiently high signal-to-noise ratio for single AP analyses has been possible. With an adenovirus-based transduction of the sensor, fast (<24 h) expression of the biosensor has been possible with a longterm persistence (we tested up to 72 h), allowing, reliable and repeated AP recordings of individual myocytes.

Our recordings are performed by a simple ratiometric read-out of two spectrally different channels. Since Mermaid is a FRET based construct this ratiometric detection is not sufficient to compensate motion artefacts induced by the contracting cells. There are two approaches to tackle this challenge: (i) Performance of measurements that determine the real or apparent FRET efficiency [34], which would require alternating excitation wavelengths. Since such a procedure is not compatible with the required acquisition speed of 1000 data points per second, we considered the alternative. (ii) Motion artefact can be pharmacologically suppressed. The most widely used substances are BDM, cytochalasin D and blebbistatin. Cytochalasin D (40 μM) presented the most severe influence of the AP (data not shown) and was therefore excluded. Blebbistatin is a specific myosin II inhibitor presenting advantages over the rather unspecific BDM, but blebbistatin was photoconverted into an inactive product within two AP recordings. Therefore Mermaid measurements and the corresponding controls using di-8-ANEPPS were performed in the presence of 20 mM BDM.

Despite the fact that the time course of the APs appeared slightly prolonged, later phases (APD_{70} and longer) could be measured reliably when compared to di-8-ANEPPS data. Such kinetic differences originate from the mechanism of voltage detection; while for di-8-ANEPPS changes in the electron distribution translate potential changes into fluorescence changes, Mermaid has to undergo a certain conformational change in order to display changes in the FRET signal. Such changes are slower. Nevertheless, quinidine displayed a clear prolongation of the AP when the membrane potential was detected with Mermaid.

The genetic coding of voltage sensors bears additional advantages, they show a higher biological inertia than small molecular dyes and speculating about the whole animal or tissue situation, expression can be restricted to specific cells and/or specific cell states [6]. In our report Mermaid displayed an even 25% higher signal in comparison to ratiometric di-8-ANEPPS recordings (cp. Fig. 5B). For a further perspective on screening genetically encoded voltage sensors refer to reference [35].

In conclusion, in this report we provide optical measurements of individual, naïve cardiac APs by a small molecular dye and a GEVS, Mermaid. Both approaches enabled us to characterise the AP time course and to quantitatively detect modulation of APD by specific pharmaceuticals. The small molecular dye as well as the biosensor will proof essential in construction and setting-up of contact-free, optical screening assays for modulation of cardiac APs such as QT-prolongation safety screens. These screens may replace a significant portion of animal experiments and pivotally contribute to cardiac safety of novel pharmaceutical developments.

Acknowledgements

This work was supported by the following German institutions: Federal Institute for Risk Assessment (BfR), German Research Foundation (DFG - KFO196) and the Federal Ministry for Education and Research (BMBF).

References

1 Arrigoni C, Crivori P: Assessment of qt liabilities in drug development. Cell Biol Toxicol 2007;23:1-13.

2 ICH: S7b nonclinical evaluation of the potential for delayed ventricular repolarization (qt interval prolongation) by human pharmaceuticals, FDA & EMEA, 2005, pp 1-10.

3 Viero C, Kraushaar U, Ruppenthal S, Kaestner L, Lipp P: A primary culture system for sustained expression of a calcium sensor in preserved adult rat ventricular myocytes. Cell Calcium 2008;43:59-71.

4 Tsutsui H, Karasawa S, Okamura Y, Miyawaki A: Improving membrane voltage measurements using fret with new fluorescent proteins. Nat Methods 2008;5:683-685.

5 Tsutsui H, Higashijima S, Miyawaki A, Okamura Y: Visualizing voltage dynamics in zebrafish heart. J Physiol 2010;588:2017-2021.

6 Hammer K, Ruppenthal S, Viero C, Scholz A, Edelmann L, Kaestner L, Lipp P: Remodelling of Ca^{2+} handling organelles in adult rat ventricular myocytes during long term culture. J Mol Cell Cardiol 2010;49:427-437.

7 Kaestner L, Scholz A, Hammer K, Vecerdea A, Ruppenthal S, Lipp P: Isolation and genetic manipulation of adult cardiac myocytes for confocal imaging. J Vis Exp 2009;31:pii: 1433. doi: 10.3791/1433.

8 Reil JC, Hohl M, Oberhofer M, Kazakov A, Kaestner L, Mueller P, Adam O, Maack C, Lipp P, Mewis C, Allessie M, Laufs U, Bohm M, Neuberger HR: Cardiac rac1 overexpression in mice creates a substrate for atrial arrhythmias characterized by structural remodelling. Cardiovasc Res 2010;87:485-493.

9 Kaestner L, Ruppenthal S, Schwarz S, Scholz A, Lipp P: Concepts for optical high content screens of excitable primary isolated cells for molecular imaging; in Licha K, Lin CP (eds): SPIE Biomedical Optics. Munich, SPIE, 2009, 7370, pp 737-745.

10 Neher RA, Mitkovski M, Kirchhoff F, Neher E, Theis FJ, Zeug A: Blind source separation techniques for the decomposition of multiply labeled fluorescence images. Biophys J 2009;96:3791-3800.

11 Huser J, Lipp P, Niggli E: Confocal microscopic detection of potential-sensitive dyes used to reveal loss of voltage control during patch-clamp experiments. Pflugers Arch 1996;433:194-199.

12 Lipp P, Huser J, Pott L, Niggli E: Subcellular properties of triggered Ca^{2+} waves in isolated citrate-loaded guinea-pig atrial myocytes characterized by ratiometric confocal microscopy. J Physiol 1996;497:599-610.

13 Bullen A, Saggau P: High-speed, random-access fluorescence microscopy: II. Fast quantitative measurements with voltage-sensitive dyes. Biophys J 1999;76:2272-2287.

14 Hardy ME, Lawrence CL, Standen NB, Rodrigo GC: Can optical recordings of membrane potential be used to screen for drug-induced action potential prolongation in single cardiac myocytes? J Pharmacol Toxicol Methods 2006;54:173-182.

15 Salata JJ, Wasserstrom JA: Effects of quinidine on action potentials and ionic currents in isolated canine ventricular myocytes. Circ Res 1988;62:324-337.

16 Milberg P, Tegelkamp R, Osada N, Schimpf R, Wolpert C, Breithardt G, Borggrefe M, Eckardt L: Reduction of dispersion of repolarization and prolongation of postrepolarization refractoriness explain the antiarrhythmic effects of quinidine in a model of short qt syndrome. J Cardiovasc Electrophysiol 2007;18:658-664.

17 Imaizumi Y, Giles WR: Quinidine-induced inhibition of transient outward current in cardiac muscle. Am J Physiol 1987;253:H704-708.

18 Wu L, Guo D, Li H, Hackett J, Yan GX, Jiao Z, Antzelevitch C, Shryock JC, Belardinelli L: Role of late sodium current in modulating the proarrhythmic and antiarrhythmic effects of quinidine. Heart Rhythm 2008;5:1726-1734.

19 Trudeau MC, Warmke JW, Ganetzky B, Robertson GA: Herg, a human inward rectifier in the voltage-gated potassium channel family. Science 1995;269:92-95.

20 Spector PS, Curran ME, Keating MT, Sanguinetti MC: Class iii antiarrhythmic drugs block herg, a human cardiac delayed rectifier K^+ channel. Open-channel block by methanesulfonanilides. Circ Res 1996;78:499-503.

21 Wang Z, Fermini B, Nattel S: Effects of flecainide, quinidine, and 4-aminopyridine on transient outward and ultrarapid delayed rectifier currents in human atrial myocytes. J Pharmacol Exp Ther 1995;272:184-196.

22 Gautier M, Hyvelin JM, de Crescenzo V, Eder V, Bonnet P: Heterogeneous kv1 function and expression in coronary myocytes from right and left ventricles in rats. Am J Physiol Heart Circ Physiol 2007;292:H475-482.

23 Lundby A, Mutoh H, Dimitrov D, Akemann W, Knopfel T: Engineering of a genetically encodable fluorescent voltage sensor exploiting fast ci-vsp voltage-sensing movements. PLoS ONE 2008;3:e2514.

24 Perron A, Mutoh H, Launey T, Knopfel T: Red-shifted voltage-sensitive fluorescent proteins. Chem Biol 2009;16:1268-1277.

25 Baker BJ, Lee H, Pieribone VA, Cohen LB, Isacoff EY, Knopfel T, Kosmidis EK: Three fluorescent protein voltage sensors exhibit low plasma membrane expression in mammalian cells. J Neurosci Methods 2007;161:32-38.

26 West JM, Stephenson DG: Contractile activation and the effects of 2,3-butanedione monoxime (bdm) in skinned cardiac preparations from normal and dystrophic mice (129/rej). Pflugers Arch 1989;413:546-552.

27 Muller O, Tian Q, Zantl R, Kahl V, Lipp P, Kaestner L: A system for optical high resolution screening of electrical excitable cells. Cell Calcium 2010;47:224-233.

28 Hirota M, Ohtani H, Hanada E, Sato H, Kotaki H, Uemura H, Nakaya H, Iga T: Influence of extracellular K^+ concentrations on quinidine-induced K^+ current inhibition in rat ventricular myocytes. J Pharm Pharmacol 2000;52:99-105.

29 Nuss HB, Marban E: Electrophysiological properties of neonatal mouse cardiac myocytes in primary culture. J Physiol 1994;479:265-279.

30 Wang L, Duff HJ: Developmental changes in transient outward current in mouse ventricle. Circ Res 1997;81:120-127.

31 Wang LJ, Sobie EA: Mathematical model of the neonatal mouse ventricular action potential. Am J Physiol Heart Circ Physiol 2008;294:H2565-2575.

32 Staudacher I, Schweizer PA, Katus HA, Thomas D: Herg: Protein trafficking and potential for therapy and drug side effects. Curr Opin Drug Discov Devel 2010;13:23-30.

33 The sicilian gambit. A new approach to the classification of antiarrhythmic drugs based on their actions on arrhythmogenic mechanisms. Task force of the working group on arrhythmias of the european society of cardiology. Circulation 1991;84:1831-1851.

34 Salonikidis PS, Zeug A, Kobe F, Ponimaskin E, Richter DW: Quantitative measurement of camp concentration using an exchange protein directly activated by a camp-based fret-sensor. Biophys J 2008;95:5412-5423.

35 Kaestner L, Tian Q, Lipp P: Action potentials in heart cells; in Jung G (ed): Fluorescent proteins - from fundamental research to bioanalytics. Heidelberg, Berlin, New York, Springer, 2011, in press.